

# The $K_0^*(800)$ scalar resonance from Roy-Steiner representations of $\pi K$ scattering

S. Descotes-Genon<sup>a</sup> and B. Moussallam<sup>b</sup>

<sup>a</sup> *Laboratoire de Physique Théorique,  
CNRS/Univ. Paris-Sud 11 (UMR 8627), 91405 Orsay Cedex, France*

<sup>b</sup> *Institut de Physique Nucléaire,  
CNRS/Univ. Paris-Sud 11 (UMR 8608), 91406 Orsay Cedex, France*

## Abstract

We discuss the existence of the light scalar meson  $K_0^*(800)$  (also called  $\kappa$ ) in a rigorous way, by showing the presence of a pole in the  $\pi K \rightarrow \pi K$  amplitude on the second Riemann sheet. For this purpose, we study the domain of validity of two classes of Roy-Steiner representations in the complex energy plane. We prove that one of them is valid in a region sufficiently broad in the imaginary direction. From this representation, we compute the  $l = 0$  partial wave in the complex plane with neither additional approximation nor model dependence, relying only on experimental data. A scalar resonance with strangeness  $S = 1$  is found with the following mass and width:  $M_\kappa = 658 \pm 13$  MeV and  $\Gamma_\kappa = 557 \pm 24$  MeV.

One striking aspect of hadron spectroscopy is the extreme scarcity of exotics, i.e., states which fail to be understood as either  $Q\bar{Q}$  or  $QQQ$  in the naive quark model. It is only recently that several such mesons have been unambiguously identified in the heavy quark sector (e.g. [1, 2]). While these are very narrow states, one expects from large- $N_c$  considerations [3] that many exotic mesons, on the contrary, should be rather wide, which makes them difficult to be singled out experimentally. From the theoretical point of view, resonances can be defined in a robust and process-independent way without assumptions on the value of the width, as a pole in the  $S$  matrix on the second Riemann sheet with respect to the elastic cut (e.g. [4]). In order to locate wide resonances in a reliable way, one must determine the value of  $S$  matrix elements in the complex energy plane, which requires a careful exploitation of analyticity properties in association with available experimental data.

In the light quark sector, the scalar mesons lighter than 1 GeV have been suspected to be exotics for a long time [5]. In this context, it is important to confirm the existence of the lightest ones, namely the  $f_0(600)$  with strangeness  $S = 0$  and the  $K_0^*(800)$  with  $S = 1$ , also familiarly called  $\sigma$  and  $\kappa$ . New indications on the presence of these resonances have been reported based on the data of the E791 [6, 7] and BES collaborations [8] (see also [9, 10]) concerning the decays  $D^+ \rightarrow \pi^- \pi^+ \pi^+$ ,  $D^+ \rightarrow K^- \pi^+ \pi^+$  and  $J/\Psi \rightarrow \pi^+ \pi^- \omega$ ,  $J/\Psi \rightarrow K^+ \pi^- K^+ \pi^-$  respectively. Conclusions were drawn from fits to the corresponding Dalitz plots with Breit-Wigner-like parametrisations. In such parametrisations, however, the presence of a pole is assumed from the start and the description of the amplitude in the complex plane is afflicted by well-known blemishes (spurious poles, absence of left-hand cuts. . .). In this paper, we address the question of the existence of a pole corresponding to the  $K_0^*(800)$  without relying on such approximations. Should this pole exist, one ought to be able to locate it in the amplitudes for  $D$  or  $J/\Psi$  decays as well as in the amplitude for elastic  $\pi K$  scattering. Recently, the existence of the  $\sigma$  meson has been confirmed in the  $\pi\pi$  scattering amplitude and its mass and width have been determined quite accurately [11] and we are following the same kind of method.

The elastic  $\pi\pi$ - and  $\pi K$ -scattering amplitudes enjoy rather unique properties because pions and kaons are the lightest particles in the QCD spectrum. The analytic structure of the amplitudes is simple, free from anomalous thresholds, and elastic unitarity holds in both direct and crossed channels in the low-energy region. An additional useful property of the  $S$  matrix element for elastic scattering is that a resonance manifests itself not only as a *pole* on the second Riemann sheet, but also as a *zero* on the first sheet.

Earlier works performing extrapolations of the  $\pi K$  scattering amplitude in the complex plane have often relied on approximations and sometimes involved model-dependent hypotheses. Cherry and Pennington [12] have used a method based on conformal mapping and stabilised fit to the data [13]. Ignoring the contributions from the left-hand cuts, they were inconclusive about the presence of a pole with  $\text{Re}(M) < 0.83$  GeV but ruled out a pole at higher mass. Their result apparently contradicts the earlier claim by Ishida et al. [14] who, using a naive Breit-Wigner parametrisation of the  $\pi K$ -scattering data, found a pole with  $\text{Re}(M) \simeq 0.88$  GeV. In refs. [15, 16] a novel dispersive representation of the partial wave  $S$  matrix was developed, which also satisfies the elastic unitarity relation

at low energy by construction. An approximation made by these authors consists in using chiral perturbation theory (ChPT) at order  $p^4$  in order to compute the discontinuities along the left-hand cuts (we will comment on the validity of this approximation in sec. 1.3). This dispersive construction does yield a  $\kappa$  resonance pole in the  $S$  matrix. Models for the scattering amplitudes of pseudoscalar mesons have been proposed by starting from their chiral expansions at leading or next-to-leading order, later improved by applying a unitarisation ansatz (see e.g. [17] for a recent review on this subject). The  $K_0^*(800)$  resonance has been discussed within this framework in refs. [18, 19]. Arguments based on unitarity bounds applied to a tree-level construction of the amplitude have been proposed in ref. [21].

In this paper, we will show that the existence of the  $K_0^*(800)$ , corresponding to a pole in the  $S$  matrix, can be established using *a*) the available experimental data and *b*) general properties of analyticity, unitarity and crossing symmetry of two-body scattering amplitudes. We will rely on dispersive representations of the Roy-Steiner (RS) type [22] for the  $I = \frac{1}{2}$   $\pi K$   $S$ -wave amplitude without performing any further approximation. In this approach, the unitarity condition on the real axis (below the inelastic threshold) is not automatically satisfied. It is rather implemented as an equation which must be solved together with those arising from the dispersive representation and from the boundary conditions. This procedure yields the phase shifts in the energy region below  $s_{match} \simeq 1$  GeV<sup>2</sup>. More precisely, in this energy range where elastic unitarity is assumed to hold to a high precision, a set of six equations is derived, involving  $\pi K \rightarrow \pi K$  and  $\pi\pi \rightarrow K\bar{K}$  partial waves with  $l = 0, 1$ . The higher partial waves ( $l \geq 2$ ) and the values for higher energies  $s \geq s_{match}$  must be provided as an input. These equations were re-analysed recently in ref. [23] using all the available data from high-statistics experiments [24, 25, 26, 27] (earlier work can be found in refs. [28, 29]).

Dispersive representations of scattering amplitudes have a limited range of validity and it is important to check whether the putative resonance falls within this domain. We will discuss this point in some detail below. It will turn out that the particular form of RS representation which was considered in ref. [23] on the real energy axis is not valid in a sufficiently large domain in the complex energy plane. A variant will be shown adequate, and we will discuss the existence, position and features of the  $K_0^*(800)$  pole in this context.

## 1 Two Roy-Steiner representations of $\pi K$ scattering and their domains of validity

### 1.1 Fixed- $t$ representation

$\pi K$  scattering is described by two different amplitudes  $F^+(s, t)$  and  $F^-(s, t)$  which are even and odd respectively under  $s$ - $u$  exchange ( $s, t, u$  being the standard Mandelstam variables). We first start with the representation proposed in ref. [23]. Since the discussion is identical for the two amplitudes, we focus on  $F^+$  and write a dispersion relation at fixed

$t$  with two subtractions (as required from the Froissart bound)

$$F^+(s, t) = c^+(t) + \frac{1}{\pi} \int_{m_+^2}^{\infty} ds' \left[ \frac{1}{s' - s} + \frac{1}{s' - u} - \frac{2s' - 2\Sigma - t}{\lambda_{s'}} \right] \text{Im}_s F^+(s', t) \quad (1)$$

with

$$m_{\pm} = m_K \pm m_{\pi}, \quad \Sigma = m_K^2 + m_{\pi}^2, \quad \lambda_{s'} = (s' - m_+^2)(s' - m_-^2) \quad (2)$$

and  $\text{Im}_s$  denotes the discontinuity along the  $s$  cut divided by  $2i$ . From the LSZ formula [30], the representation (1) can be shown to be valid in a finite region of  $t$  in a rigorous way [31, 32]. The range of validity is determined by the possibility to define the discontinuity function  $\text{Im}_s F^+(s', t)$  in the whole integration region of  $s'$  through the partial wave expansion

$$\text{Im}_s F^+(s', t) \equiv 16\pi \sum_l (2l + 1) \text{Im}_s f_l^+(s') P_l(z(s', t)) \quad (3)$$

where the argument of the Legendre polynomial is given by

$$z(s', t) = 1 + \frac{2s't}{\lambda_{s'}}. \quad (4)$$

As shown by Lehmann [33], the series of Legendre polynomials (3) converges when  $z(s', t)$  lies inside an ellipse whose focal points are located at  $z(s', t) = \pm 1$  and whose boundary touches the nearest singularity of  $\text{Im}_s F^+(s', t)$ .

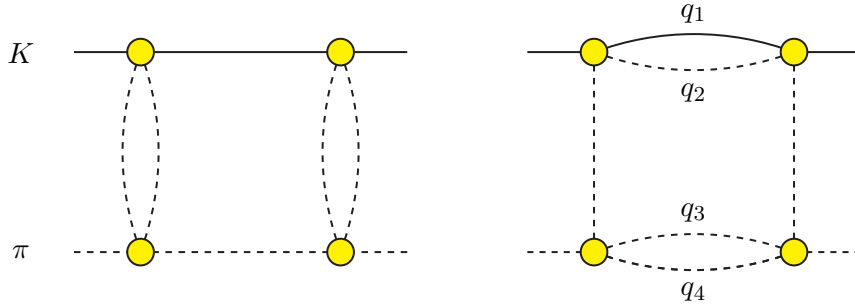


Figure 1: *Diagrams showing the contributions of the lightest particles in the  $s$ -channel and the  $t$ -channel unitarity relations for the  $\pi K$  scattering amplitude. Dashed lines correspond to  $\pi$  mesons, whereas solid lines represent  $K$  mesons.*

We assume that the scattering amplitude satisfies Mandelstam's double spectral representation [34], so that the nearest singularity is given by the boundary of the support of the double spectral functions  $\rho_{st}$ ,  $\rho_{us}$ . We recall that these boundaries are generated by considering the lightest contributions in the unitarity relations. For instance, in the case of  $\pi K$  scattering, the  $st$  boundary comes from the contributions illustrated in fig. 1. It may be written as  $t = T_{st}(s)$  with<sup>1</sup>

$$T_{st}(s) = 16m_{\pi}^2 + \frac{64m_{\pi}^4 s}{(s - (m_K - m_{\pi})^2)(s - (m_K + m_{\pi})^2)} \quad \text{when } s \leq s_0$$

<sup>1</sup>The formulae given in ref. [23] correspond to pion-nucleon scattering with  $m_N$  simply replaced by  $m_K$  which is incorrect. Using the right expressions yields only small numerical modifications to the domains of validity on the real axis quoted in ref. [23].

$$T_{st}(s) = 4m_\pi^2 + \frac{32m_\pi^3(m_K + m_\pi)}{(s - (m_K + 3m_\pi)^2)} \text{ when } s \geq s_0 \quad (5)$$

with  $s_0 = m_K^2 + 4m_K m_\pi + 5m_\pi^2 + 2m_\pi(5m_K^2 + 12m_K m_\pi + 8m_\pi^2)^{\frac{1}{2}}$ .

The expression for the boundary associated with the  $us$  spectral function can be put in the form  $t = T_{us}(s)$  with

$$\begin{aligned} T_{us}(s) &= \frac{-16m_\pi^2 m_+^2}{s - (m_K + m_\pi)^2} - s + m_+(m_K - 7m_\pi) \text{ when } s \leq s_0 \\ T_{us}(s) &= \frac{-16m_\pi^2 m_+^2}{s - (m_K + 3m_\pi)^2} - s + (m_K - m_\pi)^2 \text{ when } s \geq s_0 . \end{aligned} \quad (6)$$

In the complex  $t$  plane, the dispersive representation (1) is restricted by the  $st$  double spectral function to a domain of validity with the following boundary, expressed in polar coordinates:

$$T(\theta) = \min_{m_+^2 \leq s' \leq \infty} T_{s'}(\theta) \quad \text{with} \quad T_{s'}(\theta) = \frac{T_{st}(s')(\lambda_{s'} + s' T_{st}(s'))}{\lambda_{s'} \cos^2 \frac{\theta}{2} + s' T_{st}(s')} . \quad (7)$$

A RS representation is generated by projecting eq. (1) on the  $l = 0$  partial wave,

$$f_0^+(s) = \frac{s}{16\pi\lambda_s} \int_{-\frac{\lambda_s}{s}}^0 dt F^+(s, t) . \quad (8)$$

This projection can be performed only if the segment of integration remains inside the region of validity (7). The boundary of the domain of validity of the RS representation in the  $s$ -plane is therefore obtained, in parametric form, by solving

$$\lambda_s + s T(\theta) \exp(i\theta) = 0 . \quad (9)$$

The result is displayed in fig. 2 where the two cuts along the real axis as well as the circular cut of the partial wave amplitude are also drawn. As can be seen on this figure, the validity region of the Roy-Steiner representation based on fixed- $t$  dispersion relation gets squeezed when  $\text{Re}(s)$  is close to the  $\pi K$  threshold, which makes it a priori unfit to search for a wide resonance like the  $\kappa$ .

## 1.2 Fixed- $us$ representation

Let us now investigate a second kind of dispersion relation, sometimes called hyperbolic, in which the product  $us$  is kept fixed [23]. Setting  $us = b$ , we get a representation for  $F^+(s, t)$  of the following form:

$$\begin{aligned} F^+(s, t_b(s)) &= f^+(b) + t_b(s) h^+(b) \\ &+ \frac{1}{\pi} \int_{m_+^2}^\infty ds' \left[ \frac{2s' - 2\Sigma + t_b(s)}{(s' - s)(s' - b/s)} - \frac{2s' - 2\Sigma - t_b(s)}{s'^2 - 2\Sigma s' + b} \right] \text{Im}_s F^+(s', t_b(s')) \\ &+ \frac{t_b(s)^2}{\pi} \int_{4m_\pi^2}^\infty \frac{dt'}{t'^2(t' - t_b(s))} \text{Im}_t F^+(s'_b(t'), t') \end{aligned} \quad (10)$$

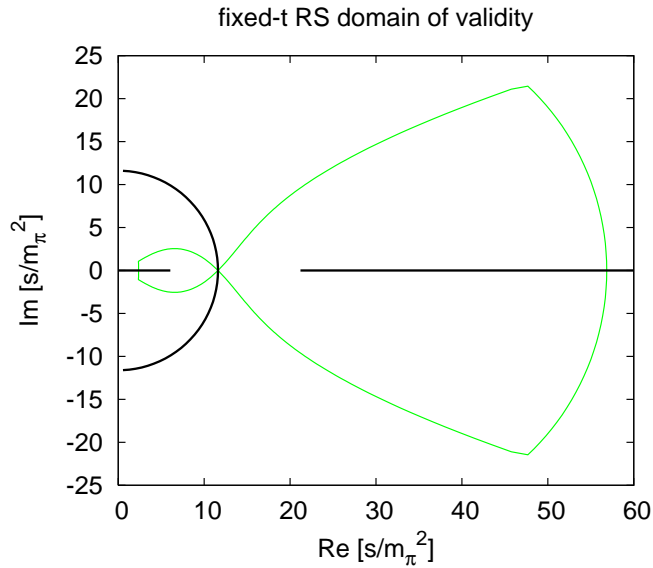


Figure 2: Domain of validity of the Roy-Steiner representation based on fixed- $t$  dispersion relation. The energy variable  $s$  is expressed in units of  $m_{\pi^+}^2$ .

with

$$t_b(s) = 2\Sigma - s - \frac{b}{s}, \quad s'_b(t') = \frac{1}{2} \left( 2\Sigma - t' + \sqrt{(2\Sigma - t')^2 - 4b} \right). \quad (11)$$

Expanding the discontinuities in partial waves and projecting the whole representation on the  $l = 0$  partial wave yields a RS representation which we denote  $\text{RS}_b$  and which is different from the fixed- $t$  representation considered earlier.

Let us now consider the domain of validity of this new representation. We must ensure that the discontinuity functions  $\text{Im}_s F^+(s', t_b(s'))$  and  $\text{Im}_{t'} F^+(s'_b(t'), t')$  are defined inside the  $s'$  and the  $t'$  integration ranges, once these functions are expanded on  $\pi K \rightarrow \pi K$  and  $\pi\pi \rightarrow K\bar{K}$  partial waves respectively. As done before, we consider each Mandelstam boundary ( $st$  and  $us$ ) and we determine the region for the parameter  $b$  inside which the representation (10) is valid. Let us denote  $B(\theta)$  the description (in polar coordinates) for the boundary of such a region. The  $S$ -wave component of this representation is then taken through

$$f_0^+(s) = \frac{1}{16\pi\lambda_s} \int_{\Delta^2}^{(2\Sigma-s)s} db F^+ \left( s, 2\Sigma - s - \frac{b}{s} \right). \quad (12)$$

The segment of integration (i.e., its end at  $(2\Sigma - s)s$ ) must remain within the region of validity in  $b$ , so that the boundary in the  $s$  plane for the  $\text{RS}_b$  representation is obtained as a solution to

$$s^2 - 2\Sigma s + B(\theta) \exp(i\theta) = 0. \quad (13)$$

The domains of validity which result from the consideration of the  $s'$  and  $t'$  integrals are shown in fig. 3. In the case of the  $t'$  integral, the  $st$  Mandelstam boundary is the only one relevant. In the case of the  $s'$  integral, one must consider both the  $us$  and the

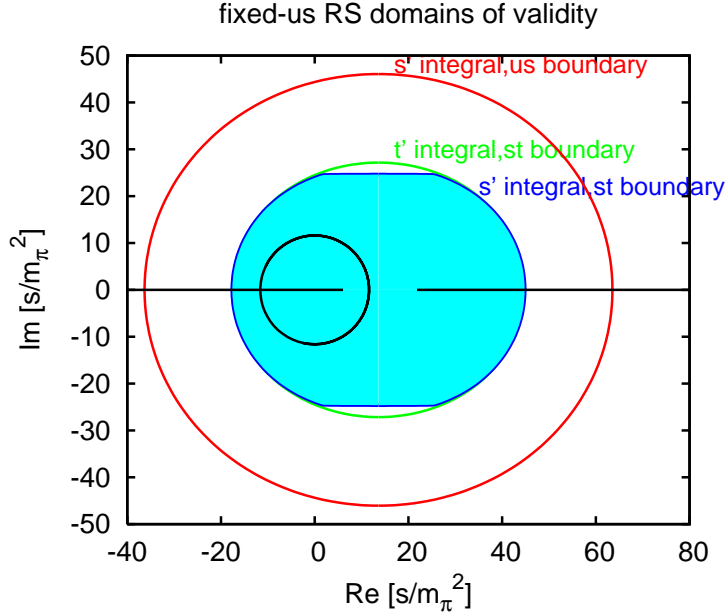


Figure 3: Domains of validity associated with the  $s'$  and  $t'$  integrals in the fixed- $us$  representation (10) and resulting from the conditions that the Lehmann ellipses do not touch the  $st$  or the  $us$  Mandelstam boundaries.

$st$  Mandelstam boundaries. The last domain is included into all the others and therefore defines the region in the complex plane where the  $RS_b$  representation is valid. The shape of this domain is quite different from fig. 2 corresponding to the fixed- $t$  RS representation. The latter exhibits a more extended validity along the real axis, whereas the former is significantly broader along the imaginary direction. Indeed, the domain of validity for  $RS_b$  extends up to  $\text{Im}(s) \simeq 0.39 \text{ GeV}^2$  when  $\text{Re}(s)$  is close to the threshold, which will turn out to be sufficient for the  $K_0^*(800)$  resonance.

### 1.3 The $RS_b$ representation of the scalar partial wave

Let us give more details on the representation of the  $f_0^{\frac{1}{2}}$  partial wave. The functions  $f^+(b)$  and  $h^+(b)$  which appear in eq. (10) have been determined in ref. [23]. Carrying out the projection of the amplitudes  $F^+$  and  $F^-$  in the form (10), we obtain the  $\pi K \rightarrow \pi K$  amplitude of isospin  $I = 1/2$  for the partial wave  $l = 0$ ,

$$\begin{aligned}
f_0^{\frac{1}{2}}(s) &= \frac{1}{2}m_+a_0^{\frac{1}{2}} + \frac{1}{12}m_+(a_0^{\frac{1}{2}} - a_0^{\frac{3}{2}}) \frac{(s - m_+^2)(5s + 3m_-^2)}{(m_+^2 - m_-^2)s} \\
&+ \frac{1}{\pi} \int_{m_+^2}^{\infty} ds' \sum_{l=0}^{\infty} \left\{ K_{0l}^{\frac{1}{2}}(s, s') \text{Im} f_l^{\frac{1}{2}}(s') + K_{0l}^{\frac{3}{2}}(s, s') \text{Im} f_l^{\frac{3}{2}}(s') \right\} \\
&+ \frac{1}{\pi} \int_{4m_\pi^2}^{\infty} dt' \sum_{l=0}^{\infty} \left\{ K_{02l}^0(s, t') \text{Im} g_{2l}^0(t') + K_{02l+1}^1(s, t') \text{Im} g_{2l+1}^1(t') \right\} , \quad (14)
\end{aligned}$$

where  $a_0^I$  denote the scattering lengths. This is the key expression which will enable us to compute the amplitude  $f_0^{\frac{1}{2}}(s)$  for complex values of  $s$ . The first few of the kernels which act on the  $\pi K \rightarrow \pi K$  partial waves  $f_l^I(s')$  read

$$\begin{aligned} K_{00}^{\frac{1}{2}}(s, s') &= \frac{1}{s' - s} - \frac{1}{3}L(s, s') - \frac{4s(s' + 2s - 3\Sigma) - 3\lambda_s}{6s\lambda_{s'}} \\ K_{01}^{\frac{1}{2}}(s, s') &= \left(1 + \frac{2(ss' - \Delta^2)}{\lambda_{s'}}\right) L(s, s') - \frac{2s(s' + s) + 3\lambda_s}{2s\lambda_{s'}} \\ K_{00}^{\frac{3}{2}}(s, s') &= \frac{4}{3}L(s, s') - \frac{8s(s' - s) + 3\lambda_s}{6s\lambda_{s'}} \end{aligned} \quad (15)$$

with

$$L(s, s') = \frac{s}{\lambda_s} \left( \log(s' + s - 2\Sigma) - \log\left(s' - \frac{\Delta^2}{s}\right) \right) \quad (16)$$

and

$$\Delta = m_K^2 - m_\pi^2, \quad \Sigma = m_K^2 + m_\pi^2. \quad (17)$$

We quote a few of the kernels which act on the  $\pi\pi \rightarrow K\bar{K}$  partial waves  $g_l^I(t')$

$$\begin{aligned} K_{00}^0(s, t') &= \frac{1}{\sqrt{3}} \left\{ \hat{L}(s, t') - \frac{1}{t'} \right\} \\ K_{01}^1(s, t') &= \frac{3\sqrt{2}}{4} \left\{ (2s - 2\Sigma + t')\hat{L}(s, t') + \frac{-5s^2 + 2\Sigma s + 3\Delta^2}{4t's} - 1 \right\} \end{aligned} \quad (18)$$

with

$$\hat{L}(s, t') = \frac{s}{\lambda_s} \log\left(1 + \frac{\lambda_s}{st'}\right). \quad (19)$$

A few comments are in order at this point:

- In the formula (14), the integrands are evaluated using the description of  $\pi K$  scattering (and its crossed channel) along the real axis obtained by solving Roy-Steiner equations [23].

More precisely, whenever the integration variables  $s', t'$  are larger than approximately 1 GeV<sup>2</sup>, the imaginary parts  $\text{Im} f_l^I(s')$ ,  $\text{Im} g_l^I(t')$  are taken from fits to the experimental data (see [23] for more details). In practice, experimental information is available for values of  $l$  up to  $l = 5$  and in a range of energies up to  $s'_{max} \simeq t'_{max} \simeq 6$  GeV<sup>2</sup>. The integrals involved here converge quickly and we restrict ourselves to values of  $s$  such that  $|s| \lesssim 1$  GeV<sup>2</sup>. We can conclude that we only need qualitative estimates for the imaginary parts in the higher integration region. For this purpose, the simple Regge pole models used in ref. [23] are appropriate.

In the lower parts of the integration ranges,  $\text{Im} f_l^I(s')$ ,  $\text{Im} g_l^I(t')$  with  $l = 0, 1$  are taken from the solutions of the RS equations computed in [23]. The scattering lengths  $a_0^{\frac{1}{2}}$  and  $a_0^{\frac{3}{2}}$  were also obtained from these solutions

$$a_0^{\frac{1}{2}} = (0.224 \pm 0.022)m_\pi^{-1}, \quad a_0^{\frac{3}{2}} = (-0.448 \pm 0.077)10^{-1}m_\pi^{-1}. \quad (20)$$



When  $s$  is on the real axis with  $m_+^2 \leq s \leq s_{match}$ , we have verified that  $f_l^I(s)$  with  $l = 0, 1$  as given from the  $RS_b$  representation do satisfy the unitarity relation to a good approximation. In other terms, these amplitudes satisfy both the RS and the  $RS_b$  equations.

- The discontinuities of the amplitude  $f_0^{\frac{1}{2}}(s)$  are generated from the pole  $1/(s' - s)$  and from the logarithmic functions  $L(s, s')$  and  $\widehat{L}(s, t')$  present in the kernels. For illustration, let us consider the discontinuity along the circular cut. Across a point  $s = \Delta \exp(i\theta)$  belonging to the circle, the discontinuity is easily computed from eq. (14) (noticing that the circular cut is contained inside the domain of validity of this representation) to be

$$f_0^{\frac{1}{2}}((\Delta - \epsilon)e^{i\theta}) - f_0^{\frac{1}{2}}((\Delta + \epsilon)e^{i\theta}) = \frac{2i}{4m_\pi^2 + 4(m_K^2 - m_\pi^2) \sin^2 \frac{\theta}{2}} \times \quad (21)$$

$$\int_{4m_\pi^2}^{4m_\pi^2 + 4\Delta \sin^2 \frac{\theta}{2}} dt' \left\{ \frac{\sqrt{3}}{3} \text{Im} g_0^0(t') - \frac{3\sqrt{2}}{4} (-2\Delta e^{i\theta} + 2\Sigma - t') \text{Im} g_1^1(t') + \dots \right\} .$$

This expression highlights the region of the circle where one is allowed to compute the discontinuity using ChPT, i.e., replacing the imaginary part of the  $\pi\pi \rightarrow K\bar{K}$  partial waves by their chiral expansions (as done in [15, 16]). The chiral expansion is expected to converge in a range  $\sqrt{t'} \lesssim 0.5$  GeV: this corresponds to the forward portion of the circle with  $-52 \lesssim \theta \lesssim 52$  degrees. Similar expressions can be derived without difficulty for the discontinuities along the left-hand cuts on the real axis. Again, it is easy to see that ChPT is applicable over a small portion of the cut and not, in particular, close to the point  $s = 0$ .

## 2 The lightest scalar resonance in $\pi K$ scattering

Phase-shift analyses for  $\pi K \rightarrow \pi K$  scattering have been performed based on high-statistics production experiments in refs. [24, 25]. For instance, fig. 4 recalls the  $l = 0$  phase of the amplitude  $\pi^+ K^- \rightarrow \pi^+ K^-$  given in ref. [25]. The phase displays a typical resonance-like behaviour in connection with the  $K_0^*(1340)$  but no similar behaviour occurs in relation with the lighter  $K_0^*(800)$ . In fact, it is difficult to immediately draw any definite conclusion from these data, since the experimental information does not quite cover the energy region which would be of interest for the  $K_0^*(800)$  resonance. In order to decide on the existence of this resonance one must combine the experimental data with theoretical constraints. Roy-Steiner representations provide such constraints by embedding information on the analyticity structure, unitarity along the real axis as well as crossing symmetry for the  $\pi K$  scattering amplitude. As discussed above, one such representation yields  $f_0^{\frac{1}{2}}(s)$  in the complex region of  $s$  shown in fig.3, which lies on the first Riemann sheet with respect to all the cuts. Let us recall here the well-known result that the elastic  $S$  matrix element

$$S_l^{\frac{1}{2}}(s) = 1 - 2 \frac{\sqrt{(m_+^2 - s)(s - m_-^2)}}{s} f_l^{\frac{1}{2}}(s) \quad (22)$$

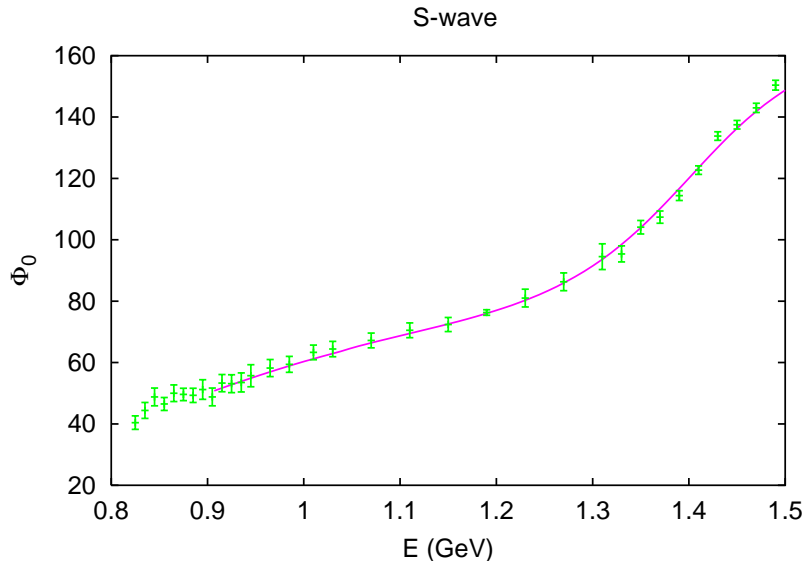


Figure 4: *Experimental values for the S-wave phases of the amplitude for charged  $\pi K$  scattering measured in ref. [25].*

exhibits a resonance as a zero on the first sheet as well as as a pole on the second sheet. This fortunate property stems from the unitarity relation which can be recast, using the analyticity properties, as an equation between the values of the amplitude on both sides of the cut

$$f_l^{\frac{1}{2}}(s - i\epsilon) - f_l^{\frac{1}{2}}(s + i\epsilon) = 2i \frac{\sqrt{(s - m_+^2)(s - m_-^2)}}{s} f_l^{\frac{1}{2}}(s + i\epsilon) f_l^{\frac{1}{2}}(s - i\epsilon) . \quad (23)$$

This relation holds for real values of  $s$  along the elastic cut below the first inelastic threshold. It can be translated into a relation for the  $S$  matrix

$$S_l^{\frac{1}{2}}(s + i\epsilon) S_l^{\frac{1}{2}}(s - i\epsilon) = 1 . \quad (24)$$

Introducing a variable  $z = -\sqrt{m_+^2 - s}$  which maps the first sheet of the  $s$  plane onto the upper part of the  $z$  plane, we can rewrite eq. (24) as

$$S_l^{\frac{1}{2}}(z) S_l^{\frac{1}{2}}(-z) = 1 . \quad (25)$$

The relation (25) holds on a finite portion of the positive real axis. By analytic continuation, it must also hold everywhere in the complex  $z$  plane. This relation immediately shows that a resonance pole  $z_0$  on the second Riemann sheet [ $\text{Im}(z_0) < 0$ ] is automatically associated to a zero at  $-z_0$ , which lies on the first sheet. Computing  $S_0^{\frac{1}{2}}(s)$  from the  $\text{RS}_b$  representation described above for the central values of our experimental input, we find that it does have a zero,  $S_0^{\frac{1}{2}}(s_0) = 0$  with

$$s_0 = 0.356 + i \cdot 0.366 \text{ GeV}^2 . \quad (26)$$

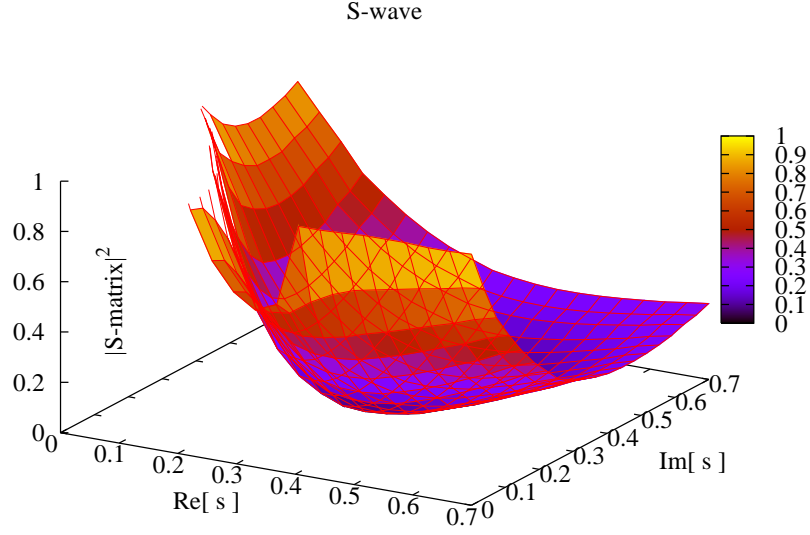


Figure 5: Plot of  $|S_0^{\frac{1}{2}}(s)|^2$  for complex values of  $s$  (in units of  $\text{GeV}^2$ ), computed from the  $\text{RS}_b$  representation (14).

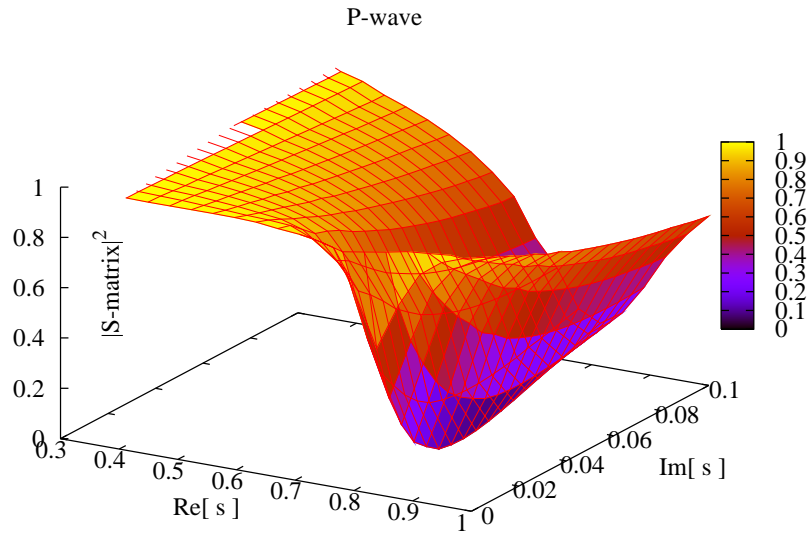


Figure 6: Same as fig. 5 showing  $|S_1^{\frac{1}{2}}|^2$ .

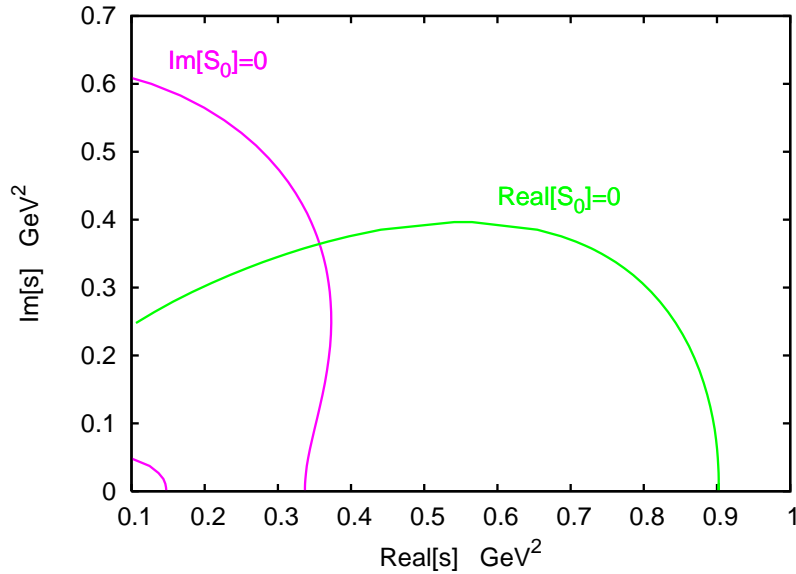


Figure 7: Lines  $L_R$  and  $L_I$  in the complex  $s$ -plane along which  $\text{Re} S_0^{\frac{1}{2}}(s)$  and  $\text{Im} S_0^{\frac{1}{2}}(s)$  vanish respectively.

The global shape of the  $S$  matrix for complex values of  $s$  is illustrated in fig. 5, which displays the squared modulus of  $S_0^{\frac{1}{2}}(s)$  resulting from our computation. The figure shows that the modulus is constant and equal to one over a portion of the real axis (in accordance with unitarity) and drops when one leaves this axis, eventually becoming zero at  $s = s_0$ . We notice the similarity of the global behaviour of the  $S$  matrix with the case of an ordinary narrow resonance. Indeed, fig. 6 shows the squared modulus of the  $P$ -wave  $S$  matrix computed using the same apparatus, which exhibits the well-known  $K^*(890)$  resonance as a zero. According to these results, the existence of the  $K_0^*(800)$  scalar resonance is established on the same footing as that of the vector  $K^*(890)$  resonance.

However, one may highlight a difference between the two situations that is illustrated in fig. 7. In the complex  $s$ -plane are drawn the two lines  $L_R$  and  $L_I$  defined as the curves along which the real and imaginary parts of the  $l = 0$   $S$  matrix vanish respectively (the point  $s_0$  corresponds to the intersection of these two lines). The line  $L_R$  starts from the real axis at the point where the phase shift is equal to  $\pi/4$  (since  $\text{Re}(S_0^I) = \cos(2\delta_0^I)$ ). In the case of an ordinary resonance, the line  $L_I$  would start from the real axis at the point where the phase shift reaches  $\pi/2$ , whereas it starts from a point situated slightly below the elastic cut in the case of the  $K_0^*(800)$ .

As stated earlier, the point  $s_0$  is located inside the domain of validity of the  $\text{RS}_b$  representation. This is illustrated in fig. 8 which shows the one-sigma error ellipse on  $s_0$  computed by varying the parameters describing our input data (see ref. [23] for more detail). In addition the figure shows that  $s_0$  is located at about the same distance from the physical cut as from the circular cut. This feature confirms that a representation of the amplitude accounting for the left-hand cuts correctly is needed in order to determine

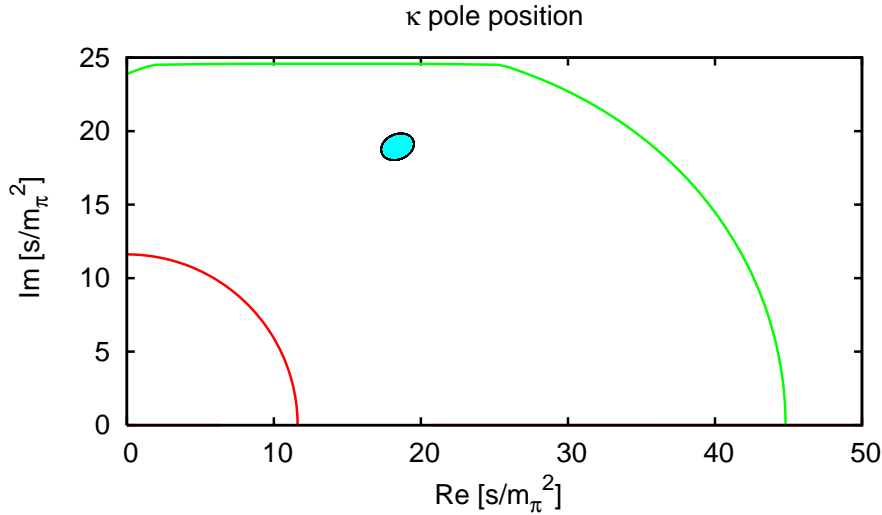


Figure 8: Position of the  $\kappa$  pole  $s_0$  and its one-sigma error ellipse (in units of  $m_\pi^2$ ). We also show the boundary of the region of validity of the  $RS_b$  representation and the left-hand cuts of the amplitude.

$s_0$  in a reliable way. The mass and width of the  $\kappa$  resonance, as defined from the square root of  $s_0$ ,  $M_\kappa + i \cdot \Gamma_\kappa/2 = \sqrt{s_0}$ , are then found to be

$$M_\kappa = 658 \pm 13 \text{ MeV}, \quad \Gamma_\kappa = 557 \pm 24 \text{ MeV}. \quad (27)$$

The errors are rather small and of the same size as the errors affecting the  $\sigma$ -meson mass and width as obtained in ref. [11]. This reflects the good quality of the experimental data used as input (see e.g. fig. 4) which is exploited in an optimal way. However, since the point  $s_0$  is not located very far from the boundary of the region of validity, one may wonder whether a significant uncertainty might be introduced by truncating the partial-wave series in the various integrands. As a matter of fact, this is unlikely, because the  $RS$  representations are expected not to break down in an abrupt way when the validity boundary is crossed. Let us consider the diagrams associated with the Mandelstam regions for  $\pi K$  scattering used to determine the validity boundary. The  $st$  boundary corresponds to setting the invariants  $(q_1 + q_2)^2$  and  $(q_3 + q_4)^2$  to their threshold values, see fig. 1. The actual dispersive representation of the amplitude is expected to involve weight functions that should be suppressed at threshold (in particular due to chiral symmetry) and that should be peaked for values of  $(q_1 + q_2)^2$  and  $(q_3 + q_4)^2$  in the resonance region (corresponding to an effectively more distant Mandelstam boundary). Because of these effects, crossing the validity boundary should affect the accuracy of the Roy-Steiner representations in a mild way : one has to venture much deeper into the complex plane to notice a significant breakdown of the dispersion relations. As an illustration, we have computed the position of the zero,  $s_0$ , using the fixed- $t$  Roy-Steiner representation. Using this dispersion relation

significantly outside of its strict domain of validity, we have found a difference of only 0.5 % in the pole position in comparison with the result from the  $RS_b$  representation.

In table 1 we summarise the results of a few other determinations of the  $K_0^*(800)$  resonance parameters in the recent literature. These are derived from input experimental data on  $\pi K$  scattering, except for the result of Aitala et al. [7] which is based on  $D \rightarrow K\pi\pi$  decays and the one from Bugg [10] who uses the same data combined with BESS II data on  $J/\psi \rightarrow K^*(890)K\pi$ . Our results are compatible with those of [15, 16] who have also employed dispersive methods. The mass which we find is lighter than in previous calculations. A similar effect was observed in ref. [11] in the case of the  $\sigma$  and it was traced to a more complete treatment of the left-hand cuts in Roy-type representations.

	$M_\kappa$ (MeV)	$\Gamma_\kappa$ (MeV)
This work	$658 \pm 13$	$557 \pm 24$
Zhou, Zheng [16]	$694 \pm 53$	$606 \pm 89$
Jamin et al. [18]	708	610
Aitala et al. [7]	$721 \pm 19 \pm 43$	$584 \pm 43 \pm 87$
Pelaez [19]	$750 \pm 18$	$452 \pm 22$
Bugg [9]	$750^{+30}_{-55}$	$684 \pm 120$
Ablikim et al. [20]	$841 \pm 23^{+64}_{-55}$	$618 \pm 52^{+55}_{-87}$
Ishida et al. [14]	$877^{+65}_{-30}$	$668^{+235}_{-110}$

Table 1: *The mass and width of the  $K_0^*(800)$  from our work and some other recent determinations. Refs. [7, 20, 14] quote Breit-Wigner parameters from which we have computed the corresponding pole positions.*

### 3 Summary and outlook

It is quite likely that many exotic mesons (or baryons) exist in QCD which are not seen simply because they have a very large width. In the case of the  $\kappa$  meson, we have demonstrated that it is perfectly possible to prove the existence of such particles by combining experimental data with some general theoretical constraints. Previously, the same conclusion was derived in the case of the  $\sigma$  meson [11]. A major advantage of the methods used here and in ref. [11] lies in the control of their range of validity as one moves away from the physical energy region into the complex plane. No such control exists for naive parametrisations of the Breit-Wigner type or even for more sophisticated ones like chiral-unitarised approaches.

The  $\pi K$ -scattering matrix in the  $S$  wave has been computed in the complex energy plane using a Roy-Steiner dispersive representation. It is worth noting that in such a representation, one must inject much more experimental information than just the  $S$ -wave phase shifts (such as data on other  $\pi K$  and crossed-channel partial waves and the high energy behaviour). Moreover, the available  $S$ -wave data does not cover the lower energy range. In this region, unitarity provides extra information which can be combined with

the RS representation to compensate for the lack of experimental data. The combination of experimental and theoretical information leads to a zero of the  $S$  matrix on the first sheet, and therefore a pole on the second one, which confirms the existence of the  $K_0^*(800)$  resonance. We have observed that the behaviour of the  $S$  matrix when the energy variable  $s$  becomes complex is qualitatively the same as in the case of a narrow resonance: the  $S$  matrix makes no difference between an ordinary and an exotic meson.

In ref. [11] the following results were found for the  $\sigma$  meson

$$M_\sigma = 441_{-8}^{+16} \text{ MeV}, \quad \Gamma_\sigma = 544_{-25}^{+18} \text{ MeV}. \quad (28)$$

Comparing  $M_\kappa$  and  $M_\sigma$  suggests that the  $\kappa$  meson is the  $S = 1$  partner of the  $\sigma$  meson. This tends to disfavour the scenario proposed by Minkowski and Ochs [35] in which the  $\sigma$  contains a sizable glueball component. If one formed a nonet by associating together the  $\sigma$ , the  $\kappa$ , the iso-singlet  $f_0(980)$  and the iso-triplet  $a_0(980)$ , its mass pattern would be clearly at variance with the usual  $Q\bar{Q}$  picture (which is also what is expected in the large  $N_c$  limit of QCD). In contrast, it would be conspicuously similar to the pattern predicted by Jaffe from a  $Q^2\bar{Q}^2$  picture a long time ago [5]. The correct values for the widths seem more difficult to reproduce in simple quark models [36]. Many different models, multiplet assignments and interpretations of the light scalar mesons have been proposed in the literature (see [37] for a review). In the future, model-independent information is expected from lattice simulations of QCD, which start to provide quantitative predictions on scalar mesons and should give further insights into this long-standing issue [38].

## Acknowledgments

We would like to thank D.V. Bugg for encouragement and correspondence. Instructive conversations with H. Leutwyler and G. Colangelo are also gratefully acknowledged.

This work is supported in part by the EU RTN contract HPPRN-CT-2002-00311 (EU-RIDICE) and the European Community-Research Infrastructure Activity under the FP6 "Structuring the European Research Area" programme (HadronPhysics, contract number RII3-CT-2004-506078)

## References

- [1] B. Aubert *et al.* [BABAR Collaboration], Phys. Rev. Lett. **90** (2003) 242001 [hep-ex/0304021].
- [2] S. K. Choi *et al.* [Belle Collaboration], Phys. Rev. Lett. **91** (2003) 262001 [hep-ex/0309032].
- [3] G. 't Hooft, Nucl. Phys. B **72** (1974) 461.
- [4] J. R. Taylor, *Scattering theory*, Wiley, New York (1972).

- [5] R. L. Jaffe, Phys. Rev. D **15** (1977) 267.
- [6] E. M. Aitala *et al.* [E791 Collaboration], Phys. Rev. Lett. **86** (2001) 770 [hep-ex/0007028].
- [7] E. M. Aitala *et al.* [E791 Collaboration], Phys. Rev. Lett. **89** (2002) 121801 [hep-ex/0204018].
- [8] M. Ablikim *et al.* [BES Collaboration], Phys. Lett. B **598** (2004) 149 [hep-ex/0406038].
- [9] D. V. Bugg, Eur. Phys. J. A **25** (2005) 107 [Erratum-ibid. A **26** (2005) 151] [hep-ex/0510026].
- [10] D. V. Bugg, Phys. Lett. B **632** (2006) 471 [hep-ex/0510019].
- [11] I. Caprini, G. Colangelo and H. Leutwyler, Phys. Rev. Lett. **96** (2006) 132001 [hep-ph/0512364].
- [12] S. N. Cherry and M. R. Pennington, Nucl. Phys. A **688** (2001) 823 [hep-ph/0005208].
- [13] A. Nogová, J. Pišút and P. Prešnajder, Nucl. Phys. B **61** (1973) 438; A. Nogová, J. Pišút Nucl. Phys. B **61** (1973) 445.
- [14] S. Ishida, M. Ishida, T. Ishida, K. Takamatsu and T. Tsuru, Prog. Theor. Phys. **98** (1997) 621 [hep-ph/9705437].
- [15] H. Q. Zheng, Z. Y. Zhou, G. Y. Qin, Z. G. Xiao, J. J. Wang and N. Wu, Nucl. Phys. A **733** (2004) 235 [hep-ph/0310293].
- [16] Z. Y. Zhou and H. Q. Zheng, hep-ph/0603062.
- [17] J. A. Oller, E. Oset and A. Ramos, Prog. Part. Nucl. Phys. **45** (2000) 157 [hep-ph/0002193].
- [18] M. Jamin, J. A. Oller and A. Pich, Nucl. Phys. B **587** (2000) 331 [hep-ph/0006045].
- [19] J. R. Pelaez, Phys. Rev. Lett. **92** (2004) 102001 [hep-ph/0309292], J. R. Pelaez, Mod. Phys. Lett. A **19** (2004) 2879 [hep-ph/0411107].
- [20] M. Ablikim *et al.* [BES Collaboration], Phys. Lett. B **633** (2006) 681 [hep-ex/0506055].
- [21] D. Black, A. H. Fariborz, F. Sannino and J. Schechter, Phys. Rev. D **58** (1998) 054012 [hep-ph/9804273].
- [22] S. M. Roy, Phys. Lett. B **36** (1971) 353; F. Steiner, Fortsch. Phys. **19** (1971) 115.
- [23] P. Büttiker, S. Descotes-Genon and B. Moussallam, Eur. Phys. J. C **33** (2004) 409 [hep-ph/0310283].



- [24] P. Estabrooks, R. K. Carnegie, A. D. Martin, W. M. Dunwoodie, T. A. Lasinski and D. W. Leith, Nucl. Phys. B **133** (1978) 490.
- [25] D. Aston *et al.*, Nucl. Phys. B **296** (1988) 493.
- [26] D. Cohen, D. S. Ayres, R. Diebold, S. L. Kramer, A. J. Pawlicki and A. B. Wicklund, Phys. Rev. D **22** (1980) 2595.
- [27] A. Etkin *et al.*, Phys. Rev. D **25** (1982) 1786.
- [28] J. P. Ader, C. Meyers and B. Bonnier, Phys. Lett. B **46** (1973) 403.
- [29] N. Johannesson and G. Nilsson, Nuovo Cim. A **43** (1978) 376.
- [30] H. Lehmann, K. Symanzik and W. Zimmermann, Nuovo Cim. **1** (1955) 205.
- [31] S. Mandelstam, Nuovo Cim. **15** (1960) 658.
- [32] A. Martin, Nuovo Cim. **A42** (1966) 930, **A 44** (1966) 1219.
- [33] H. Lehmann, Nuovo Cim. **10** (1958) 579.
- [34] S. Mandelstam, Phys. Rev. **112** (1958) 1344.
- [35] P. Minkowski and W. Ochs, Eur. Phys. J. C **9** (1999) 283 [[hep-ph/9811518](#)].
- [36] L. Maiani, F. Piccinini, A. D. Polosa and V. Riquer, Phys. Rev. Lett. **93** (2004) 212002 [[hep-ph/0407017](#)].
- [37] C. Amsler and N. A. Tornqvist, Phys. Rept. **389** (2004) 61.
- [38] C. McNeile and C. Michael [UKQCD Collaboration], Phys. Rev. D **74** (2006) 014508 [[hep-lat/0604009](#)].